Magnetic Resonance in Medicine 57:859–865 (2007)

Fast Mapping of the T_2 Relaxation Time of Cerebral Metabolites Using Proton Echo-Planar Spectroscopic Imaging (PEPSI)

Shang-Yueh Tsai,[1] Stefan Posse,[2,3] Yi-Ru Lin,[4] Cheng-Wen Ko,[5] Ricardo Otazo,[3] Hsiao-Wen Chung,[1*] and Fa-Hsuan Lin[6,7,8]

Metabolite T_2 is necessary for accurate quantification of the absolute concentration of metabolites using long-echo-time (TE) acquisition schemes. However, lengthy data acquisition times pose a major challenge to mapping metabolite T_2. In this study we used proton echo-planar spectroscopic imaging (PEPSI) at 3T to obtain fast T_2 maps of three major cerebral metabolites: N-acetyl-aspartate (NAA), creatine (Cre), and choline (Cho). We showed that PEPSI spectra matched T_2 values obtained using single-voxel spectroscopy (SVS). Data acquisition for 2D metabolite maps with a voxel volume of 0.95 ml (32 × 32 image matrix) can be completed in 25 min using five TEs and eight averages. A sufficient spectral signal-to-noise ratio (SNR) for T_2 estimation was validated by high Pearson's correlation coefficients between logarithmic MR signals and TEs (R^2 = 0.98, 0.97, and 0.95 for NAA, Cre, and Cho, respectively). In agreement with previous studies, we found that the T_2 values of NAA, but not Cre and Cho, were significantly different between gray matter (GM) and white matter (WM; $P < 0.001$). The difference between the T_2 estimates of the PEPSI and SVS scans was less than 9%. Consistent spatial distributions of T_2 were found in six healthy subjects, and disagreement among subjects was less than 10%. In summary, the PEPSI technique is a robust method to obtain fast mapping of metabolite T_2. Magn Reson Med 57:859–865, 2007. © 2007 Wiley-Liss, Inc.

Key words: proton echo-planar spectroscopic imaging; single-voxel spectroscopy; T_2 relaxation time; cerebral metabolites; gray/white matter difference

Estimation of the relaxation times of metabolites is necessary for accurate quantification of metabolite concentrations using long-echo-time (TE) acquisition schemes (1–3). Given the *T*2 relaxation time, metabolite signals acquired at different TEs can be extrapolated to obtain the signal at TE = 0 and thus estimate the concentration of the metabolite (4). Differences in *T*2 decay are negligible only for short-TE methods (with TE below 10 ms). In several pathological conditions, such as edema and ischemic stroke (5–8), interactions between cerebral metabolites and macromolecules and proteins are known to modify the biochemical environments of the metabolites, which in turn alters the motion-sensitive *T*2 relaxation time. Accurate estimation of metabolite *T*2 is therefore especially important in clinical applications of magnetic resonance spectroscopy (MRS) to ascertain whether changes in metabolite MR signals are derived from fluctuations in the metabolite concentration or from changes in the metabolite relaxation time (2,9). In addition to providing information about metabolite concentration, *T*2 values may give complementary information about metabolite behavior, as has been suggested by studies of brain tumor (9), ischemic stroke (5–7,10), virus infection (11), drug abuse (12), and other neurological disorders (13–15).

The *T*2 relaxation times of metabolites can be measured by collecting multiple spectra over a range of TEs and then fitting the MR signals as a function of TE (1–3,5,10). Several studies have reported metabolite *T*2 values in various brain regions at different field strengths. Most of these studies used the single-voxel spectroscopy (SVS) technique and reported region-specific *T*2 variations in normal brain (1–4,16). At 3T, the *T*2 values of N-acetyl-aspartate (NAA), creatine (Cre), and choline (Cho) have been reported to range from 220 ms to 301 ms, 143 ms to 178 ms, and 187 ms to 276 ms, respectively, in occipital gray (GM) and white matter (WM), cerebellum, basal ganglia, and other cortical regions (1–3). A general shortening of *T*2 relaxation time at higher field strengths has also been found (1–4,16–18). Because of inherent regional variations, acquiring whole-brain metabolite *T*2 maps in a single measurement using spectroscopic imaging (SI) techniques is very helpful for monitoring pathologically induced alterations. Unfortunately, only a few studies have employed SI techniques for *T*2 estimation (6,15,17). The major difficulty associated with using the technique is the lengthy acquisition time required for repetitive spatial encoding in two or even three spatial dimensions. For instance, completing a data acquisition for 2D chemical shift imaging (CSI) with a 32 × 32 imaging matrix and TR of 2 s takes more than 30 min for only one TE. Acquisition with multiple TEs is simply not feasible. Therefore, the devel-

[1]Department of Electrical Engineering, National Taiwan University, Taipei, Taiwan.

[2]Department of Psychiatry, University of New Mexico School of Medicine, Albuquerque, New Mexico, USA.

[3]Department of Electrical and Computer Engineering, University of New Mexico, Albuquerque, New Mexico, USA.

[4]Department of Electronic Engineering, National Taiwan University of Science and Technology, Taipei, Taiwan.

[5]Department of Computer Science and Engineering, National Sun Yat-Sen University, Kaohsiung, Taiwan.

[6]Massachusetts General Hospital-Harvard Medical School-Massachusetts Institute of Technology (MGH-HMS-MIT) Athinoula A. Martinos Center for Biomedical Imaging, Charlestown, Massachusetts, USA.

[7]Department of Radiology, Massachusetts General Hospital, Boston, Massachusetts, USA.

[8]Institute of Biomedical Engineering, National Taiwan University, Taipei, Taiwan.

Grant sponsor: National Institutes of Health; Grant numbers: R01 HD040712; R01 NS037462; R01 EB000790-04; P41 RR14075; R01 DA14178-01; Grant sponsor: Taiwan National Science Council; Grant number: NSC-95-2221-E-002-179; Grant sponsors: Mental Illness and Neuroscience Discovery Institute (MIND); Taiwan Ministry of Education.

*Correspondence to: Hsiao-Wen Chung, Ph.D., Department of Electrical Engineering, Room 238, Bldg. 2, Dept. of Electrical Engineering, National Taiwan University, No. 1, Sec. 4, Roosevelt Road, Taipei, Taiwan 10764. E-mail: chung@cc.ee.ntu.edu.tw

Received 26 October 2006; revised 24 January 2007; accepted 9 February 2007.

DOI 10.1002/mrm.21225
Published online in Wiley InterScience (www.interscience.wiley.com).

opment of fast SI techniques to measure the *T*2 relaxation times of cerebral metabolites within clinically acceptable times is highly desirable.

Over the past two decades, many fast SI techniques have been proposed, including multiple spin-echo acquisition (19), echo-planar spatial encoding (20), and spiral readout (21). Compared to the traditional CSI technique, these methods offer two- to fourfold accelerations in data acquisition time. By contrast, proton echo-planar spectroscopic imaging (PEPSI) can accelerate data acquisition by an order of magnitude using echo-planar readouts to collect spectral and 1D spatial information. The PEPSI technique has been developed for clinical MR scanners to measure 2D and 3D metabolite distributions in several minutes (22,23) and with high spatial resolution (24). Given its benefit of fast acquisition, the PEPSI technique has already been employed in many clinical studies (22,25,26).

In this work we examined the feasibility of using the PEPSI sequence on a 3T MR system to estimate the 2D spatial distributions of *T*2 relaxation times of the three major cerebral metabolites: NAA, Cre, and Cho. We aimed to optimize experimental parameters to establish a protocol that yields sufficient spectral SNR and accurate metabolic quantification. The spatial resolution achievable with PEPSI is utilized to obtain regional *T*2′s for both GM and WMs, which are then validated by SVS. The proposed protocol allows completion of scanning in 30 min, and offers the capability of mapping metabolite *T*2′s in clinical studies.

MATERIALS AND METHODS

Subjects and Data Acquisition

Six normal volunteers (three males and three females, mean age = 30 ± 10 years) were enrolled in this study. All experiments were performed on a 3T MR system (Trio; Siemens Medical Solutions, Erlangen, Germany) with an eight-channel coil array that covers the whole brain circumferentially with eight surface receive-only coils. We used the body coil for RF excitation. All in vivo experiments were conducted under the supervision of the MGH Institutional Review Board and we obtained informed consent from all study participants.

Before the MRS acquisitions, we acquired multislice axial *T*1-weighted images using a gradient-echo sequence (TR/TE/flip angle = 10 ms/2 ms/15°) for anatomy localization, as required for subsequent PEPSI and SVS experiments. We acquired 15 image slices of 4-mm thickness, with no gap, to cover the whole brain. For the shimming, we checked the resonant frequency and the width of the resonance peak on the scanner based on the existing shimming currents on the gradient coils. After the phase maps across the whole brain were measured based on the existing shimming currents, a new set of shimming currents was calculated using the manufacturer software on the scanner. This procedure was repeated until the phase map converged to the most homogeneous phase distribution.

The PEPSI sequence includes 1) water suppression using chemical shift-selective saturation (CHESS) (27), 2) application of complete eight-slice outer volume suppression along the perimeter of the brain, 3) spin-echo excitation consisting of a 90° RF pulse followed by two 180 refocusing RF pulses, and 4) fast spatial-spectral encoding of the half-echo using an EPI readout gradient train along the *x*-axis (23). Data were acquired with 1024 gradient inversions at 83.33-kHz readout bandwidth and online regridding to account for ramp sampling. Even- and odd-echo data were collected separately. The reconstructed spectral width after even/odd echo editing was 1086 Hz, with 512 complex points corresponding to a spectral resolution of 2.1 Hz. To obtain 2D spatial encoding, we applied additional phase encoding along the *y*-axis. PEPSI data were acquired from a para-axial slice at the upper edge of the ventricles with a voxel size of 0.95 ml (matrix size = 32 × 32, FOV = 220 mm, slice thickness = 20 mm). For each subject, five PEPSI data sets were collected at TEs of 50, 100, 160, 220, and 300 ms. The TR was chosen to approximate the *T*1 values of metabolites for optimization of the acquisition efficiency for signal-to-noise ratio (SNR) (28). Given previously reported *T*1 values ranging between 1000 ms and 1500 ms at 3T (2), we chose a TR of 1200 ms for this study. To enhance the SNR, we employed eight signal averages for the PEPSI acquisitions at each TE, which yielded a total scan time of 25.6 min. To investigate the possibility of further accelerating data acquisition with the use of fewer averages, and the consequential effects of reduced SNR, we performed two further experiments on one subject. In these additional studies, we reduced the number of signal averages at TEs of 50, 100, 160, and 220 ms from eight to six and four, respectively. The number of averages for 300 ms TE was not reduced, but was kept at eight to maintain the SNR of long-TE spectra. The total scan times were 20.5 and 15.4 min, respectively, for these two additional experiments.

SVS experiments were performed after the PEPSI scans using the point-resolved spectroscopy (PRESS) (29) sequence. For each subject, spectra were acquired from representative WM and GM voxels on the same slice as in the PEPSI acquisition. The locations of these two volumes of interest (VOIs) are depicted in Fig. 1. The voxel size was 8 ml (20 × 20 × 20 mm3), approximately corresponding to the nine voxels in the PEPSI scan. SVS data were collected at the same TEs and TR used for the PEPSI data. The number of signal averages was 64, and the spectral width was 1120 Hz with 512 complex points.

Postprocessing

All spectra were first processed with sinusoidal spatial filtering of the *k*-space data and 4-Hz exponential temporal filtering of the half-echo data. Following Fourier transformation from time domain to spectral domain, the spectra were phased using automatic zeroth-order phase correction. For PEPSI, spectra from even and odd echoes were averaged together to increase the SNR. A first-order polynomial baseline correction was applied over the spectral range of 1–4 ppm to attenuate baseline drift and overlap of residual water signal. The signal of each metabolite was calculated by integrating the corresponding peak.

The *T*2 relaxation times of three major cerebral metabolites (NAA, Cre, and Cho) were estimated from the integrated signal corresponding to each TE. Using a monoexponential function, the metabolite signals became a linear

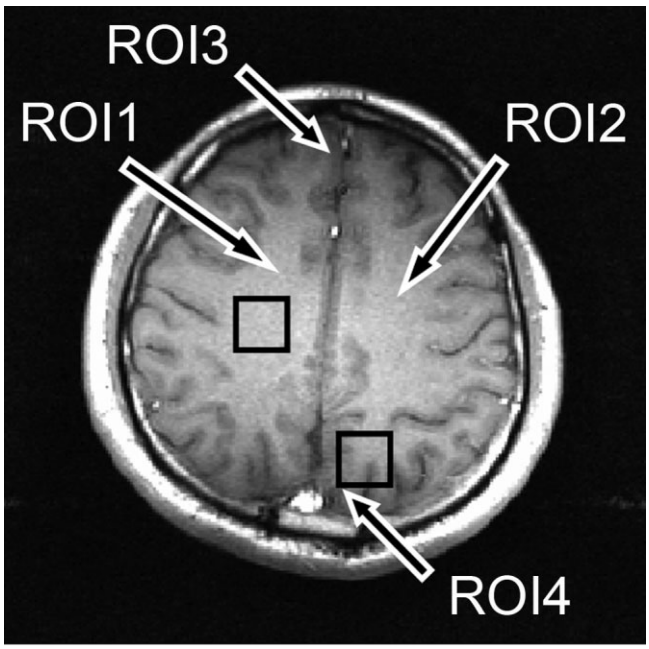

FIG. 1. T_1-weighted gradient-echo image used for localization of PEPSI and SVS experiments. The image shown here corresponds to the PEPSI imaging slice. For the SVS scans, two VOIs were defined in WM and GM (black squares). All ROIs in regional analysis were manually selected on the T_1-weighted image (their positions are indicated by arrows).

function of TE after a natural logarithm was taken. We performed linear regression using least-squares fitting. The *T*2 values of individual metabolites were thus calculated as the inverse of slope of the regression curve. Pearson's correlation coefficient (R), as an index reflecting the linearity of the semilogarithmic plot, was used to evaluate the goodness of *T*2 fit. All voxels with R2 values less than 0.9 were excluded and displayed as zero in the *T*2 map.

Statistical Analysis

To investigate the regional distribution of *T*2 values, four regions of interest (ROIs) were selected in WM areas of the left hemisphere (ROI1) and right hemisphere (ROI2), and GM areas of the frontal lobe (ROI3) and parietal lobe (ROI4) (arrows in Fig. 1). The means and standard deviations (SDs) of the metabolite *T*2 values from each ROI were calculated. We used a one-tail *t*-test to compare regional *T*2 differences between WM and GM for the three metabolites in each of these ROIs. To compare the *T*2 values of PEPSI and SVS scans, we chose two square ROIs (3×3 voxels) from the PEPSI data to match the same locations of the VOIs in the SVS data. All ROIs were selected manually from the *T*1-weighted images.

RESULTS

Representative spectra selected from a WM voxel in both PEPSI and SVS scans are shown in Fig. 2. Both the PEPSI and SVS data revealed clearly identified metabolite peaks, and the spectra baselines were relatively flat after first-order polynomial correction. The major metabolite peaks progressively decreased as the TE increased. The semilogarithmic plots of PEPSI metabolite signals vs. TE demonstrated satisfactory linearity (R^2 values ranging from 0.98 to 0.95; Fig. 3a). The SVS data also demonstrated such linearity ($R^2 > 0.99$; Fig. 3b). The averaged differences in T_2 estimates between PEPSI and SVS over the six subjects were 4%, 5%, and 9% for NAA, Cre, and Cho, respectively.

A comparison of T_2 fitting quality with different acquisition protocols is shown in Fig. 4. With eight signal averages (total scan time = 25.6 min), the averaged R^2 of the whole brain was over 0.95 for all three metabolites. R^2 decreased as the number of signal averages decreased concomitantly with SNR. Although the R^2 values remained greater than 0.90 for NAA and Cre for all three protocols, R^2 for Cho decreased to 0.87 when only four signal averages (the 15-min protocol) were used (Fig. 4).

The T_2 values estimated from our subjects ranged from 200 ms to 250 ms for NAA in the GM, 260 ms to 320 ms for NAA in the WM, 140 ms to 170 ms for Cre, and 190 ms to 270 ms for Cho (Table 1). A regional analysis showed that for NAA, T_2 values were significantly higher in the WM than in the GM ($P < 0.001$). The differences in T_2 for the GM and WMs were statistically insignificant for Cre ($P = 0.32$) and Cho ($P = 0.11$), as is directly depicted by the T_2 maps shown in Fig. 5. Our results are in agreement with those previously reported. For NAA, Cre, and Cho, Traber et al. (2) measured T_2 values of 301 ms, 178 ms, and

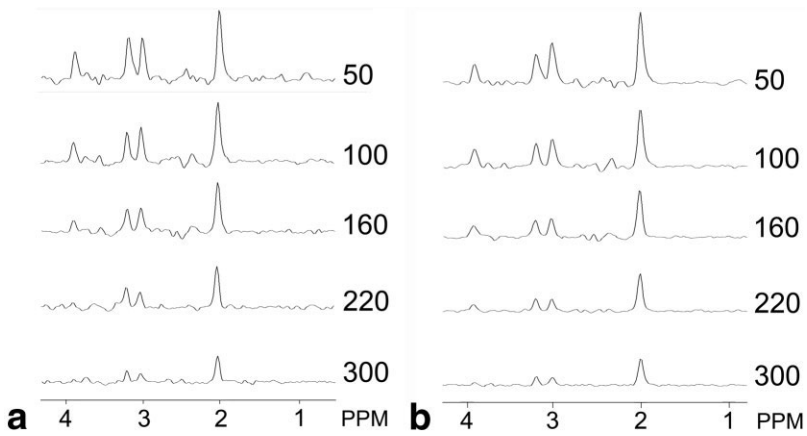

FIG. 2. Representative spectra from PEPSI (**a**) and SVS (**b**) from one subject. Baseline correction was successful in all cases. The metabolite peaks can be identified easily from the high-quality spectra.

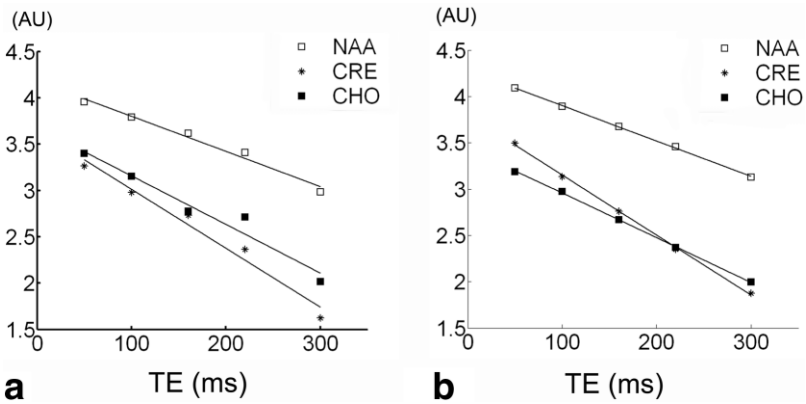

FIG. 3. Semilogarithmic plots of metabolite signal vs. TE for NAA, Cre, and Cho in PEPSI (**a**) and SVS (**b**) from representative spectra shown in Fig. 2. The R^2 values for the PEPSI data are 0.98, 0.97, and 0.95 for NAA, Cre, and Cho, respectively, with T_2 values estimated at 263, 157, and 191 ms. Data obtained from the SVS scan show better linearity given the higher SNR with larger voxel size.

222 ms, respectively, in the occipital WM, and 247 ms, 162 ms, and 222 ms in the motor cortex. Mlynarik et al. (3) estimated 247 ms, 152 ms, and 207 ms in the occipital GM, and 295 ms, 156 ms, and 187 ms in the occipital WM. Intersubject differences in metabolite T_2 values were less than 10% (Table 1), showing high consistency across the six healthy volunteers recruited in this study. The spatial distributions of T_2 for all three metabolites were also similar among our subjects (Fig. 5).

DISCUSSION

In this study we demonstrated that the spatial distribution of the T_2 values of the three major cerebral metabolites (NAA, Cre, and Cho) can be obtained in less than 30 min using the PEPSI sequence. The relatively short scanning time of the PEPSI technique increases the potential to map metabolite T_2's for both research and clinical applications. A clear difference in T_2 between the GM and WM was found for NAA ($P < 0.001$), but not for Cre and Cho, suggesting different biochemical environments in the GM and WMs, specifically for NAA. This finding matches those of previous reports that used the SVS technique to separately measure metabolite T_2 values in GM and WM (1–3). Unlike SVS, our PEPSI technique provides the ability to display the spatial distribution of T_2 values. Such T_2 mapping is especially important for pathological conditions in which specific regions of T_2 alterations may not be known prior to data acquisition.

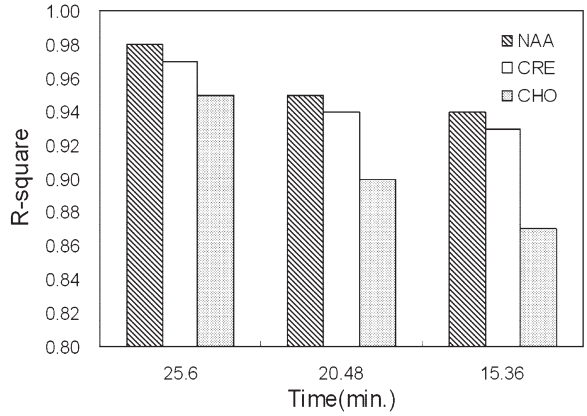

FIG. 4. R^2 values for three cerebral metabolites using different protocols in one subject. The R^2 values displayed were averaged across the whole brain. The scan time of 25.6 min corresponds to the protocol with eight averages, and 20.48 and 15.36 min correspond to the six- and four-signal averages for TEs less than 300 ms, respectively. SNR reduction resulting from fewer signal averages results in decreased fitting precision and hence lowered R^2 values.

In addition to the advantage of improved spatial resolution, T_2 values estimated from PEPSI data matched results previously observed. Compared to our SVS experiments, the PEPSI data exhibited a difference of less than 9%. The quality of data fitting is reflected by high Pearson's correlation coefficients, indicating the reliability of T_2 estimations. The T_2 maps for Cho exhibited high spatial variability, with T_2 near the central interhemispheric fissure seemingly longer than in lateral regions of the cerebral hemispheres (Fig. 5). Further interpretation of this finding may be possible with future recruitment of more subjects. The spatial variation observed for Cho T_2 may arise from its comparatively low R^2 values, which can be partially explained by the regional variation in line width and the interference of the underlying multiplets of myo-inositol and phosphooethanolamine (3).

However, even with the accuracy of metabolite T_2 estimation that is achievable with PEPSI (error less than 10% compared to SVS scans), it should be noted that the detection of pathological alterations by using metabolite T_2 values alone requires further careful investigations. Taking the best-quantified NAA as an example, the T_2 in the WM regions for subject 3 was found to be around 230–300 ms, whereas that for subject 5 was 270–350 ms (Fig. 5). Since these T_2 values, especially those within the SVS ROIs, were in good agreement with SVS estimations (261 and 299 ms for subjects 3 and 5, respectively), the intersubject difference is in part the consequence of natural variability. On the other hand, for Cho, which showed inferior SNR compared to NAA, the relatively large intrasubject variations shown in Fig. 5 could arise from a combination of natural spatial distribution and technical uncertainty. To further explore the inter- and intrasubject variability of metabolite T_2, it is necessary to obtain measurements with higher SNR. For example, using highly sensitive surface coil arrays and averaging voxels across ROIs will increase SNR. The present study shows technical feasibility and quantifies the limits of T_2 quantification with the current technology.

Table 1
List of T_2 Relaxation Times (in ms) of NAA, Cre, and Cho From Four ROIs Defined in the White Matter of the Right Hemisphere (Right WM), White Matter in the Left Hemisphere (Left WM), Gray Matter of the Frontal Lobe (Frontal GM), and Gray Matter of the Parietal Lobe, Plus Whole-Brain-Averaged T_2 and R^2 Values*

	NAA	CRE	CHO
Right WM (ROI1) (ms)	295 ± 12	156 ± 07	217 ± 17
Left WM (ROI2) (ms)	287 ± 16	152 ± 05	215 ± 19
Frontal GM (ROI3) (ms)	235 ± 18	157 ± 15	229 ± 23
Parietal GM (ROI4) (ms)	238 ± 12	155 ± 07	225 ± 26
Whole brain (ms)	262 ± 13	151 ± 05	221 ± 13
R^2	0.98 ± 0.004	0.97 ± 0.01	0.95 ± 0.01

*For each of six subjects, we calculated the mean and standard deviations of T_2 in each ROI. The intersubject variability is less than 10% for NAA and Cre, and around 10% for Cho. Note that the higher SD in T_2 values of Cho matched the lower R^2 values (Fig. 4) and the T_2 map results (Fig. 5).

Because the signal of a metabolite arises from the integration of individual spectral peaks, the accuracy of T_2 estimation can be affected by the spectral baseline. The shape of the baseline can be complex, showing overlaps by either broad spectral lines belonging to high-molecular-weight compounds, spectral multiplets with complex coupling patterns, or simple drift due to residual water and interscan fluctuations. Baseline correction is thus very im-

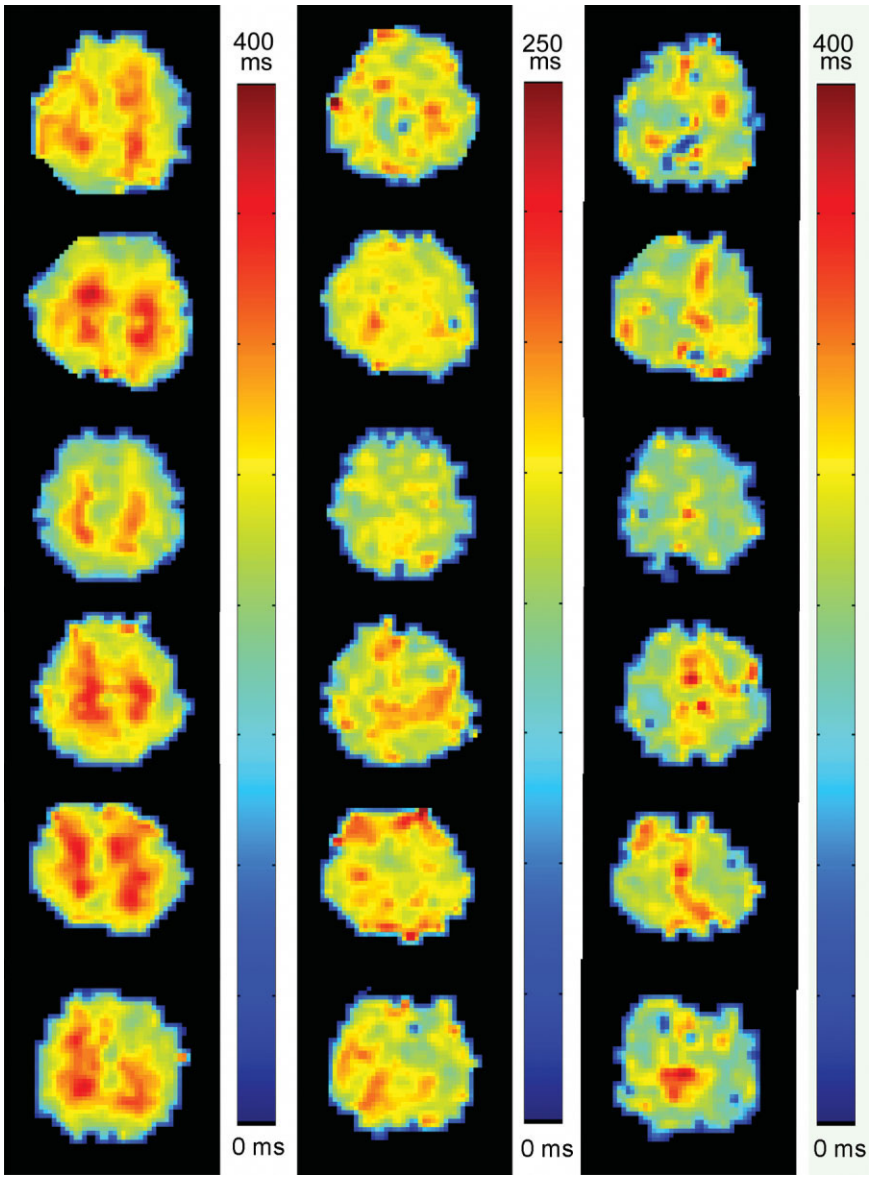

FIG. 5. *T2* maps of NAA, Cre, and Cho (left to right) from six subjects (top to bottom). The *T2* values (in milliseconds) were found to be consistent across the six subjects, with *T2* maps of Cho exhibiting a slightly increased spatial variance. Note that there is a clear difference in *T2* between the WM and GM in the NAA maps, but not in the Cre and Cho maps.

portant because metabolite peak integration is very sensitive to any baseline fluctuation. In this study, TE values larger than 50 ms were chosen to reduce the signal contributed by J-coupled multiplets and macromolecular resonances. Therefore, as shown in Fig. 2, the simple baseline correction algorithm applied in this study is sufficient to successfully correct baseline drift in relatively long-TE spectra. T_2 relaxation closely following monoexponential decay could be seen in all of the metabolites investigated (Fig. 3).

As shown in Fig. 4, the SNR is the key factor affecting the quality of T_2 relaxation time quantification. The SNR is a more critical issue for Cre and Cho than for NAA because of the intrinsically lower concentrations and shorter T_2 values of these two metabolites. This in turn implies that for these two metabolites, the signal is lower at long TEs, and more signal averages are therefore needed to maintain the SNR. In our protocol, TE ranges up to 300 ms. For a metabolite with T_2 greater than 300 ms, such as NAA in the WM, the lack of long-TE data may result in estimation errors (1). Nevertheless, in this study of PEPSI, NAA was successfully quantified with an error of less than 4% compared to the SVS results. On these grounds, the proposed PEPSI protocol should be considered acceptable. Furthermore, if spectra with longer TE (more than 300 ms) were used in the protocol, fewer signal averages must be used for spectra at short TE in order to maintain the same scanning time. Using fewer averages lowers the quality of linear fitting for Cre and Cho. Given the SNR concerns for Cre and Cho, and constraints on feasible total scanning time, extending the TE to a longer TE is not desirable in terms of acquisition efficiency. Eight signal averages were used in the proposed protocol because SNR loss resulting from a further reduction in the number of signal averages yields less accurate T_2 estimations (Fig. 4). If $R^2 = 0.95$ is used as the criterion for reliable T_2 fitting, the 20-min protocol may be a suitable faster alternative when NAA is the only metabolite of interest.

A relatively large voxel size ($20 \times 20 \times 20$ mm^3) was used for the SVS experiments. Partial volume effect due to the mixture of GM and WM may complicate calculation of T_2. In other words, we expect that the SVS T_2 values reported for NAA may reflect over- and underestimation in the GM and WM, respectively. By contrast, PEPSI provides better spatial resolution ($6.88 \times 6.88 \times 20$ mm^3 in this study) to mitigate this partial volume effect. With carefully selected ROIs from the GM and WM separately, we expect that the derived PEPSI T_2 values may reflect regional differences with higher accuracy, although possibly with a lower SNR due to the smaller voxel size (0.95 ml in PEPSI scans compared to 8 ml in SVS scans). Fortunately, with the current MR system, the 1-ml voxel size provided sufficient SNR using the eight-channel phased-array coils and signal averages (22,25). As demonstrated in our study, the errors between SVS and PEPSI experiments for identical ROIs varied by only 4–9%, implying that intersubject variability of 10% may be a consequence of interscan variability.

A primary goal of this study was to establish a protocol with a realistic scanning time and sufficient spectral SNR for quantification of metabolite relaxation times. The proposed protocol was developed for a 3T MR system. Compared with the routine clinical protocol of about 13 min (16×16 with two signal averages using conventional SI at TR = 1.5 s) (30), the 25-min protocol provides a strong rationale for T_2 mapping at the acceptable expense of 12 min of additional scan time. For lower magnetic fields (1.5T or lower), however, the reduced SNR and longer T_2 values would require more signal averages and wider TE ranges for T_2 estimation, which would lead to longer total scanning times and consequently to limited applications. Further improvements to this protocol include the use of large-*N* array coils (31), higher-field systems (32,33), and parallel imaging techniques (34). Other extensions of this approach consist of mapping T_1 relaxation time or mapping relaxation time in three dimensions, both of which are under investigation.

In conclusion, our proposed method has been demonstrated to successfully estimate the T_2 relaxation times of three major cerebral metabolites within a clinically acceptable data acquisition time. The compatibility of this method with patient examination shows strong potential for monitoring T_2 alterations accompanied by pathological changes (5,6,8–12,14,15).

ACKNOWLEDGMENTS

The authors thank Dr. Wen-Yih Issac Tseng and the National Taiwan University Hospital 3T MRI laboratory for technical support with the MR scanner. S.Y.T. received financial support from the Taiwan Ministry of Education under the international student exchange program.

REFERENCES

1. Brief EE, Whittall KP, Li DK, MacKay AL. Proton T2 relaxation of cerebral metabolites of normal human brain over large TE range. NMR Biomed 2005;18:14–18.
2. Traber F, Block W, Lamerichs R, Gieseke J, Schild HH. 1H metabolite relaxation times at 3.0 Tesla: measurements of T1 and T2 values in normal brain and determination of regional differences in transverse relaxation. J Magn Reson Imaging 2004;19:537–545.
3. Mlynarik V, Gruber S, Moser E. Proton T(1) and T(2) relaxation times of human brain metabolites at 3 Tesla. NMR Biomed 2001;14:325–331.
4. Frahm J, Bruhn H, Gyngell ML, Merboldt KD, Hanicke W, Sauter R. Localized proton NMR spectroscopy in different regions of the human brain in vivo. Relaxation times and concentrations of cerebral metabolites. Magn Reson Med 1989;11:47–63.
5. van der Toorn A, Dijkhuizen RM, Tulleken CA, Nicolay K. T1 and T2 relaxation times of the major 1H-containing metabolites in rat brain after focal ischemia. NMR Biomed 1995;8:245–252.
6. Walker PM, Ben Salem D, Lalande A, Giroud M, Brunotte F. Time course of NAA T2 and ADC(w) in ischaemic stroke patients: 1H MRS imaging and diffusion-weighted MRI. J Neurol Sci 2004;220:23–28.
7. Lei H, Zhang Y, Zhu XH, Chen W. Changes in the proton T2 relaxation times of cerebral water and metabolites during forebrain ischemia in rat at 9.4 T. Magn Reson Med 2003;49:979–984.
8. Kamada K, Houkin K, Hida K, Matsuzawa H, Iwasaki Y, Abe H, Nakada T. Localized proton spectroscopy of focal brain pathology in humans: significant effects of edema on spin-spin relaxation time. Magn Reson Med 1994;31:537–540.
9. Isobe T, Matsumura A, Anno I, Yoshizawa T, Nagatomo Y, Itai Y, Nose T. Quantification of cerebral metabolites in glioma patients with proton MR spectroscopy using T2 relaxation time correction. Magn Reson Imaging 2002;20:343–349.
10. Fujimori H, Michaelis T, Wick M, Frahm J. Proton T2 relaxation of cerebral metabolites during transient global ischemia in rat brain. Magn Reson Med 1998;39:647–650.

11. Wilkinson ID, Paley M, Chong WK, Sweeney BJ, Shepherd JK, Kendall BE, Hall-Craggs MA, Harrison MJ. Proton spectroscopy in HIV infection: relaxation times of cerebral metabolites. Magn Reson Imaging 1994;12:951–957.
12. Christensen JD, Kaufman MJ, Frederick B, Rose SL, Moore CM, Lukas SE, Mendelson JH, Cohen BM, Renshaw PF. Proton magnetic resonance spectroscopy of human basal ganglia: response to cocaine administration. Biol Psychiatry 2000;48:685–692.
13. Cady EB. Metabolite concentrations and relaxation in perinatal cerebral hypoxic-ischemic injury. Neurochem Res 1996;21:1043–1052.
14. Rooney WD, Ebisu T, Mancuso A, Graham S, Weiner MW, Maudsley AA. Metabolite 1H relaxation in normal and hyponatremic brain. Magn Reson Med 1996;35:688–696.
15. Sijens PE, Oudkerk M. 1H chemical shift imaging characterization of human brain tumor and edema. Eur Radiol 2002;12:2056–2061.
16. Choi CG, Frahm J. Localized proton MRS of the human hippocampus: metabolite concentrations and relaxation times. Magn Reson Med 1999; 41:204–207.
17. Hetherington HP, Mason GF, Pan JW, Ponder SL, Vaughan JT, Twieg DB, Pohost GM. Evaluation of cerebral gray and white matter metabolite differences by spectroscopic imaging at 4.1T. Magn Reson Med 1994;32:565–571.
18. Posse S, Cuenod CA, Risinger R, Le Bihan D, Balaban RS. Anomalous transverse relaxation in 1H spectroscopy in human brain at 4 Tesla. Magn Reson Med 1995;33:246–252.
19. Duyn JH, Moonen CT. Fast proton spectroscopic imaging of human brain using multiple spin-echoes. Magn Reson Med 1993;30:409–414.
20. Mansfield P. Spatial mapping of the chemical shift in NMR. Magn Reson Med 1984;1:370–386.
21. Adalsteinsson E, Irarrazabal P, Topp S, Meyer C, Macovski A, Spielman DM. Volumetric spectroscopic imaging with spiral-based k-space trajectories. Magn Reson Med 1998;39:889–898.
22. Posse S, Dager SR, Richards TL, Yuan C, Ogg R, Artru AA, Muller-Gartner HW, Hayes C. In vivo measurement of regional brain metabolic response to hyperventilation using magnetic resonance: proton echo planar spectroscopic imaging (PEPSI). Magn Reson Med 1997;37:858–865.
23. Posse S, Tedeschi G, Risinger R, Ogg R, Le Bihan D. High speed 1H spectroscopic imaging in human brain by echo planar spatial-spectral encoding. Magn Reson Med 1995;33:34–40.
24. Chu A, Alger JR, Moore GJ, Posse S. Proton echo-planar spectroscopic imaging with highly effective outer volume suppression using combined presaturation and spatially selective echo dephasing. Magn Reson Med 2003;49:817–821.
25. Dager SR, Friedman SD, Heide A, Layton ME, Richards T, Artru A, Strauss W, Hayes C, Posse S. Two-dimensional proton echo-planar spectroscopic imaging of brain metabolic changes during lactate-induced panic. Arch Gen Psychiatry 1999;56:70–77.
26. Dager SR, Layton ME, Strauss W, Richards TL, Heide A, Friedman SD, Artru AA, Hayes CE, Posse S. Human brain metabolic response to caffeine and the effects of tolerance. Am J Psychiatry 1999;156:229–237.
27. Haase A, Frahm J, Hanicke W, Matthaei D. 1H NMR chemical shift selective (CHESS) imaging. Phys Med Biol 1985;30:341–344.
28. Prato FS, Drost DJ, Keys T, Laxon P, Comissiong B, Sestini E. Optimization of signal-to-noise ratio in calculated T1 images derived from two spin-echo images. Magn Reson Med 1986;3:63–75.
29. Bottomley PA. Spatial localization in NMR spectroscopy in vivo. Ann NY Acad Sci 1987;508:333–348.
30. Bendszus M, Warmuth-Metz M, Klein R, Burger R, Schichor C, Tonn JC, Solymosi L. MR spectroscopy in gliomatosis cerebri. AJNR Am J Neuroradiol 2000;21:375–380.
31. Wiggins GC, Triantafyllou C, Potthast A, Reykowski A, Nittka M, Wald LL. 32-Channel 3 Tesla receive-only phased-array head coil with soccer-ball element geometry. Magn Reson Med 2006;56:216–223.
32. Posse S, Otazo R, Caprihan A, Bustillo J, Chen H, Zuo C, Renshaw P, Magnotta V, Mueller B, Lim KO, Ugurbil K, Mullins P, Gasparovic C, Alger JR. Rapid brain glutamate mapping in central and peripheral gray matter at 3 and 4 Tesla using short TE proton-echoplanar-spectroscopic-imaging (PEPSI). In Proceedings of the 14th Annual Meeting of ISMRM; Seattle, USA, 2006. p 484.
33. Posse S, Otazo R, Tsai SY, Wald LL, Lin FH. Sensitivity encoded proton echo planar spectroscopic imaging (PEPSI) in human brain at 7 Tesla. In: Proceedings of the 14th Annual Meeting of ISMRM, Seattle, WA, USA, 2006 (Abstract 3079).
34. Dydak U, Weiger M, Pruessmann KP, Meier D, Boesiger P. Sensitivity-encoded spectroscopic imaging. Magn Reson Med 2001;46:713–722.